sexhy experimental results on pressure dynamics from head-on reflections of hydrogen flames

S Koudriakov, E Studer, A Dancelme, C Tenaud, P.-A Masset

SSEXHY EXPERIMENTAL RESULTS ON PRESSURE DYNAMICS FROM HEAD-ON REFLECTIONS OF HYDROGEN FLAMES

S. Koudriakov[1], E. Studer[1], A. Dancelme[1], C. Tenaud[2], P.-A. Masset[1]

[1] Univ. Paris-Saclay, CEA, ISAS, F-91191 Gif-sur-Yvette, France
[2] Univ. Paris-Saclay, CNRS, CentraleSupélec, Laboratoire EM2C, 91190, Gif-sur-Yvette, France

Corresponding author : **sergey.kudriakov@cea.fr**

ABSTRACT

In the past few years, CEA has been fully involved at both experimental and modeling levels in projects related to hydrogen safety in nuclear and chemical industries, and has carried out a test program using the experimental bench SSEXHY (Structure Submitted to an EXplosion of HYdrogen) in order to build a database of the deformations of simple structures following an internal hydrogen explosion. Different propagation regimes of explosions were studied, varying from detonations to slow deflagrations.
During the experimental campaign, it was found that high-speed deflagrations, corresponding to relatively poor hydrogen-air mixtures, resulted in higher specimen deformation compared to those related to detonations of nearly stoichiometric mixtures. This paper explains this counter-intuitive result from qualitative and quantitative points of view. It is shown that the overpressure and impulse from head-on reflections of hydrogen flames corresponding to poor mixtures of specific concentrations could have very high values at the tube end.

1.0 INTRODUCTION

Every industry dealing with hydrogen must cope with an increased hazard of gaseous explosions, which can severely damage property and harm people. In particular, nuclear installations are at risk of hydrogen explosions during severe accidents, potentially compromising the containment of radioactive materials. The 1979 Three Mile Island accident in the United States, and more recently the 2011 Fukushima accident in Japan have both emphasized the need to understand the physical phenomena associated to the propagation and structural interactions of these explosions within nuclear installations – with the aim of ensuring safer operation and improved management during accidents.
In the past few years, CEA has been fully involved at both experimental and modelling levels in projects related to hydrogen safety in nuclear and chemical industries, such as HYINDOOR, MITHYGENE or HYTUNNEL [1], [2]. Understanding the fluid-structure interactions during an explosion of hydrogen and its consequences is one of the main tasks of all these projects.
In this context, CEA has carried out a test program using together the experimental bench SSEXHY and the CFD software EUROPLEXUS, so as to build a database of the deformations of simple structures following an internal hydrogen explosion, and propose a predictive tool to compute them. Different propagation regimes of explosions were studied, varying from detonations to slow deflagrations. Various deformable structures were tested, including plates of variable thickness and diameter. Detailed diagnostics were used to acquire sufficient data for the validation of fluid-structure numerical codes.
During the experimental campaign, it was found that high-speed deflagrations, corresponding to relatively poor hydrogen-air mixtures, resulted in higher specimen deformation compared to those related to detonations of nearly stoichiometric mixtures [3]. This counter-intuitive result showed that there was not always a monotonous relationship between fuel concentration on the lean side and total impulse during head-on impact. This result is particularly relevant for safety, because it implies that even relatively low hydrogen concentrations during accidents and/or leaner regions of gas could lead to potentially more hazardous explosions, requiring an explanation from qualitative as well as quantitative viewpoints.
In order to explain this phenomenon, a separate set of experiments where a solid flange of 5 cm thickness was installed at the end of the tube. Several pressure transducers were implanted inside the flange in

order to capture the time evolutions of pressure and impulse from head-on reflections of the waves resulting from premixed explosions of lean mixtures up to stoichiometric ones. Additionally, the influence of geometry has been studied, with either elongated tube of the same diameter, or with a diverging section placed at the end of the tube where the cross-section was enlarged by a factor of 1.67. The paper is organized as follows. The SSEXHY test facility is described in Section 2. The main results corresponding to different hydrogen/air mixtures and different adapters attached to the tube are presented in Section 3, followed by conclusions and future work description.

2.0 DESCRIPTION OF THE SSEXHY TEST FACILITY

The SSEXHY combustion tube [4] features a stainless steel obstructed duct designed to study the acceleration mechanisms of premixed hydrogen/air flames. The tube includes four interchangeable sections connected by flanges and in the present campaign, only three were used for most of experiments. Each section is 1310 mm long with an internal diameter of 120 mm. Two blank flanges can be used to seal the combustion tube at its extremities. A picture of the experimental device is shown in Figure 1.

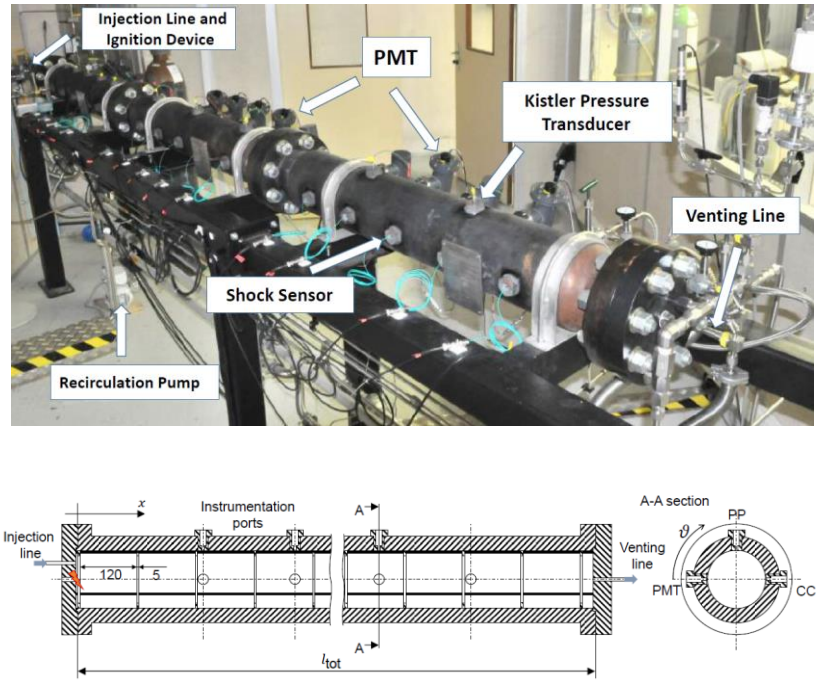

Figure 1. Picture of SSEXHY Tube having 3 sections and showing different instrumentations (top); schematic of the Tube (bottom). Sizes are given in mm. PMT="PhotoMultiplier Tube", CC = "Shock Sensor", PP = "Pressure Transducer".

The design pressure of the tube is 100 bar. The total length of the tube, l_{tot}, can vary between 3930 mm (three sections) and 5240 mm (four sections). Two blank flanges are used to seal the combustion tube at its extremities. An array of equally spaced annular obstacles is placed inside the tube in order to promote turbulence. The obstacle blockage ratio (i.e. the ratio between the area obstructed by the obstacle and the tube cross-section area) in this experimental campaign is 0.3. Three thin threaded rods form the structure supporting the obstacles. The stainless steel annular obstacles are 5 mm thick and having a 120 mm uniform pitch.

Gas injection lines are connected to one end-flange via an isolation valve. At the center of this flange, a threaded hole houses an automotive spark plug. Mixture ignition is provided by the electrical discharge

between the two electrodes of the plug; the energy released by the plug is approximately 25 mJ. On the other extremity, venting lines ensure burnt gas evacuation from the combustion tube at the end of the experiment. A primary vacuum pump is also connected at both sides of the tube.
Once hydrogen and air are injected inside the tube using partial pressure technique, a non-homogeneous mixture is formed. A gas recirculation pump (BÜHLER P2.74 ATEX pump) then promotes the homogenization. The mixture is forced to recirculate via an external loop for about 30 minutes before reaching the homogeneous condition. This period of time was calibrated from pre-tests using helium instead of hydrogen and measuring the local concentration with thermal conductivity gauges. Two taps are available for gas sampling at the recirculation loop connections to the tube wall (see Figure 2).

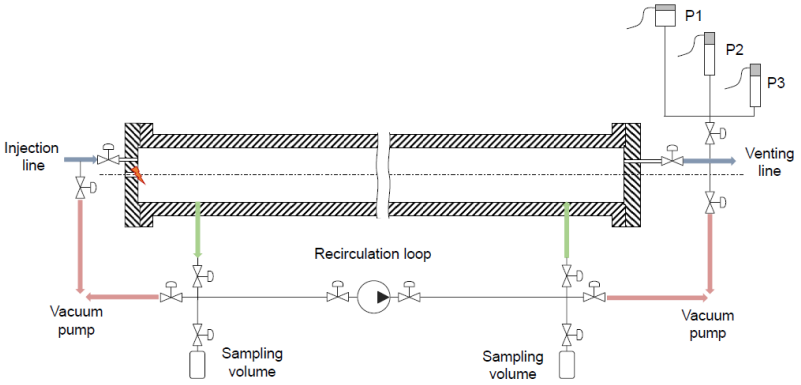

Figure 2. Injection and venting system of the combustion tube and external recirculation loop.

At the end of the homogenization process, the flammable mixture is sampled inside sampling volumes located at two extremities of the tube (Figure 2) and analysed via gas chromatography. The analysis is performed using an Agilent 490 µGC equipped with a thermal conductivity detector (TCD). Argon is used as carrier gas. This allows detecting helium, oxygen, nitrogen, hydrogen and methane in a single GC module. The absolute uncertainty on the mixture composition is lower than 0.1% ([5]).
Two types of adapters can be installed at the right end of the explosion tube (Figure 3). Each of these adapters can be used as a support for a specimen in form of a small (D = 175 mm) or big (D = 285 mm) circular plates. The cylindrical adapter (Figure 3, top) is 500 mm long and its inner diameter is equal to the tube inner diameter, i.e. 120 mm. The conical adapter (Figure 3, bottom) is 500 mm long and its inner diameter increases smoothly from 120 mm to 200 mm at the big plate fixation. Both adapters are obstacle-free.
In order to observe the behaviour of pressure waves when they are in contact with a specimen, a preliminary tests have been performed with a full solid flange at the extreme end of the each of adapters. Several pressure transducers have been installed inside each flange in order to have a cartography of the pressure evolutions (Figure 4).

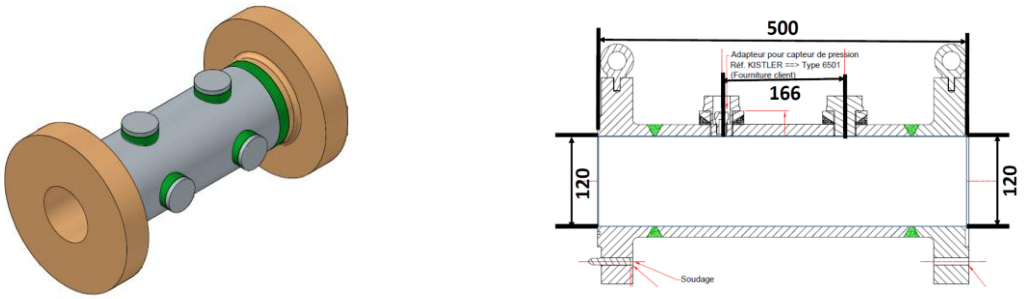

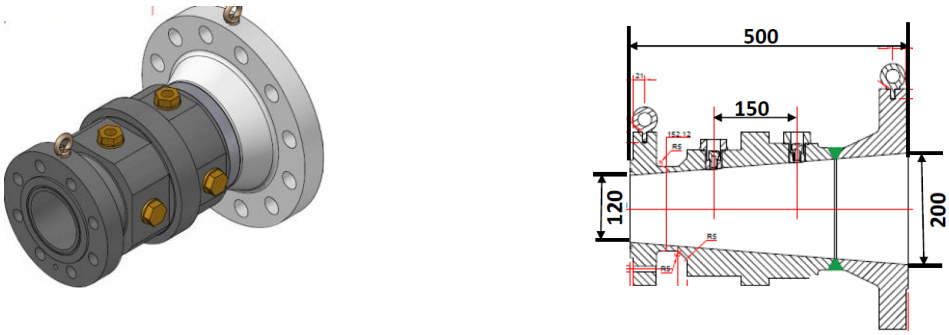

Figure 3. The adapters used for plate specimen: cylindrical (top) and conical (bottom). The dimensions are given in mm.

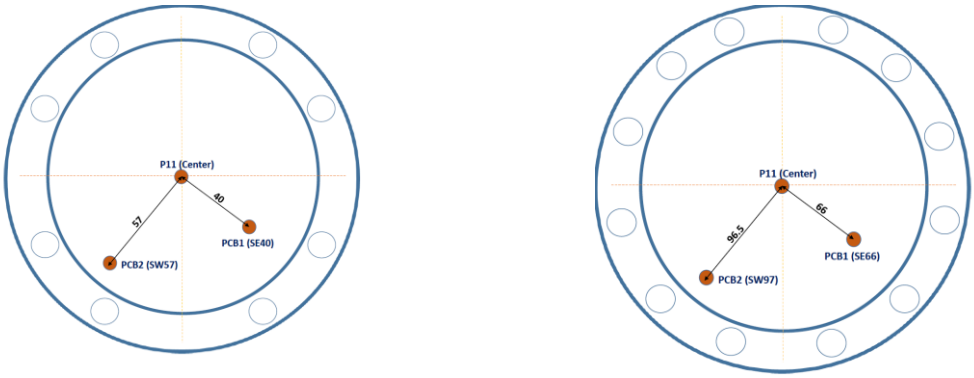

Figure 4. Pressure transducers locations on a full flange corresponding to cylindrical adapter (left) and conical adapter (right). The dimensions are given in mm.

3.0 MAIN RESULTS

In this document we present the results corresponding to the initial hydrogen molar concentrations of $X_{H2} = 15\%$, $X_{H2} = 18\%$ and $X_{H2} = 29\%$. All tests have been performed at initial pressure P = 1 bar and temperature T = 300 K. At $X_{H2} = 15\%$ the wave is represented by a decoupled shock–flame complex propagating at the speed near Chapman-Jouguet deflagration speed, while at $X_{H2} = 29\%$, the wave is a detonation wave with a cell size of approximately 2 cm. The main properties of the considered mixtures are presented in Table 1. These properties have been obtained using the COSILAB code ([6]).

Table 1. Main properties of considered mixtures (CJ = "Chapman-Jouguet).

Concentration %	Compression ratio, σ	Laminar flame speed, S_L^0 (m/s)	Laminar flame thickness, δ_L(mm)	CJ deflagration velocity (m/s)	CJ detonation velocity (m/s)
15	4.58	0.28	0.57	723	1530
18	5.14	0.59	0.42	791	1644
29	6.82	2.22	0.38	1002	1967

Flame velocity evolutions along the tube

The results for flame velocity obtained using the data from the Photomultiplier tubes are presented on Figure 5-Figure 7.

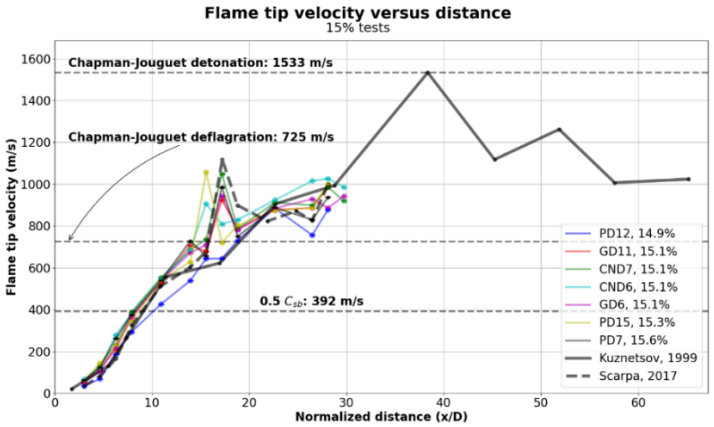

Figure 5. Flame velocity versus normalized distance, $X_{H2} \approx 15\%$.

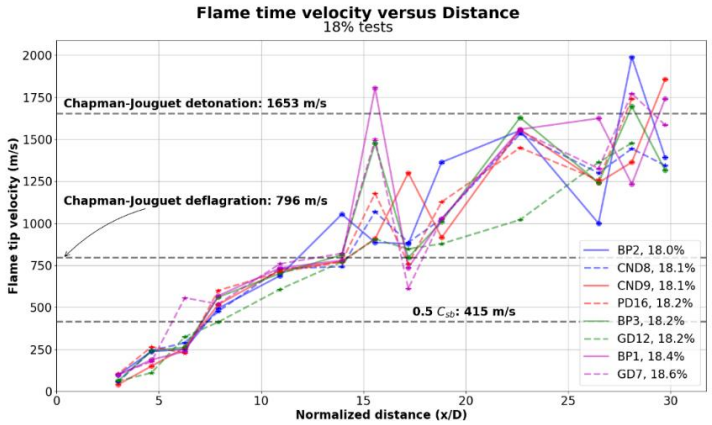

Figure 6. Flame velocity versus normalized distance, $X_{H2} \approx 18\%$.

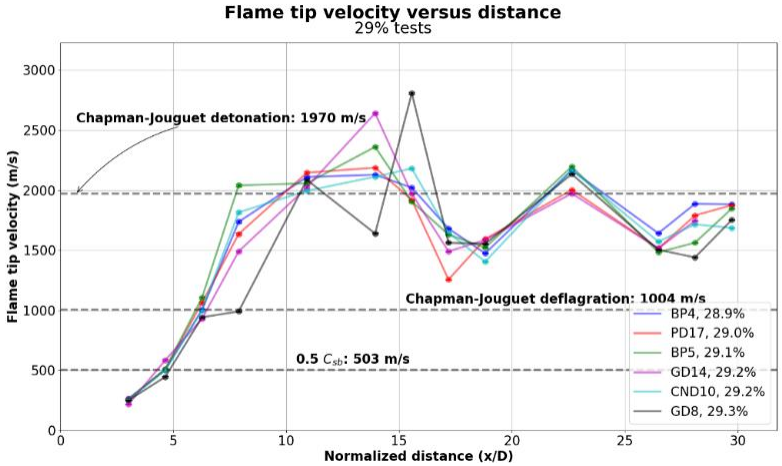

Figure 7. Flame velocity versus normalized distance, $X_{H2} \approx 29\%$.

The presented results are based on several tests performed during different test campaigns. The hydrogen concentration is systematically analysed via gas chromatography, it slightly varies around the predetermined value; the values corresponding to Chapman-Jouguet (CJ) deflagration, and detonation velocities are based on averaged concentrations for each Figure.
The flame velocities corresponding to hydrogen concentration of 15% are consistent with experimental data of [7] for most of the flame trajectory. The flame is in the fast deflagration regime, reaching half the burnt gas sonic velocity at about 1.0 meters (x/D = 8) into the set-up. The CJ deflagration speed is consistently attained at about 2.0 meters. Afterwards, the flame speed oscillates around 1000 m/s (Figure 5). Looking at the Figure 6 ($X_{H2} = 18\%$), we can see that the CJ deflagration velocity is systematically reached at 1.7 m from the ignition point (x/D=14). After that, the flame velocity continues to rise with an oscillatory behaviour, and the CJ detonation velocity is attained close to the end of the facility. In the tests corresponding to nearly stoichiometric H2-air composition (Figure 7) the fast deflagration regime is achieved at 0.6 meters (x/D = 5). Flame tip velocity increases at a relatively high rate and the CJ detonation velocity is reached at 1.2 meters (x/D = 10). The velocities then oscillate around this value until the end of the tube.
Overall, the higher the hydrogen concentration in the gas mixture, the higher is the flame velocity, increasing on average from 1000 m/s ($X_{H2} = 15\%$) to 1500 m/s ($X_{H2} = 18\%$), and to 2000 m/s ($X_{H2} = 29\%$). It is reasonable to suggest that *the more energetic mixture would create higher head-on overpressures and higher impulses*.

Pressure and Impulse evolutions at the flange: cylindrical adapter.

All pressure signals were sampled at a rate of 400 kHz and low-pass filtered at 60 kHz. In what follows, the pressure signals corresponding to the hydrogen concentration of 15% are presented in blue colour, those corresponding to 18% are presented in black colour, and the signals corresponding to the 29% - in red colour. For each concentration, the test has been performed *at least* two times.
The overpressure evolutions at the flange center (see Figure *8*) are shown on the Figure 9, where zoomed picture at the initial time is given at the right. We can see that the first pressure peaks have comparable values varying between 40 and 50 bar, while the later behavior is very different, especially if we look at the evolution corresponding to 15% hydrogen concentration. There are several pressure oscillations of relatively high amplitude reaching 68 bar, which 40% higher than the maximum overpressure corresponding to the detonation wave, $X_{H2} = 29\%$. The oscillation period is close to 0.1 ms, which corresponds to wave velocity of 1200 m/s if we take as a length scale the tube diameter.

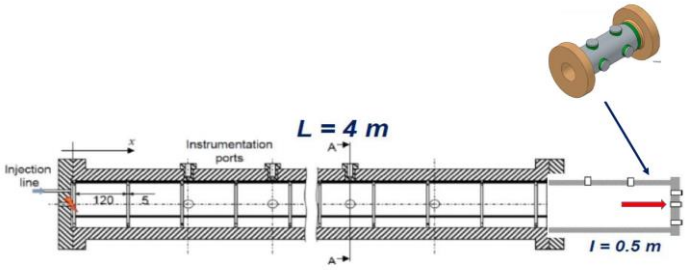

Figure 8. Sketch of the SSEXHY facility with cylindrical adapter and a full flange equipped with pressure transducers.

Alongside with the overpressure evolution we present the impulse *I(t)* evolution, with

$$I(t) = \int_0^t (p(t') - p_0)\, dt' \quad (1)$$

Time 0 for each pressure evolution is defined as the arrival of the shock/detonation wave at the solid flange.

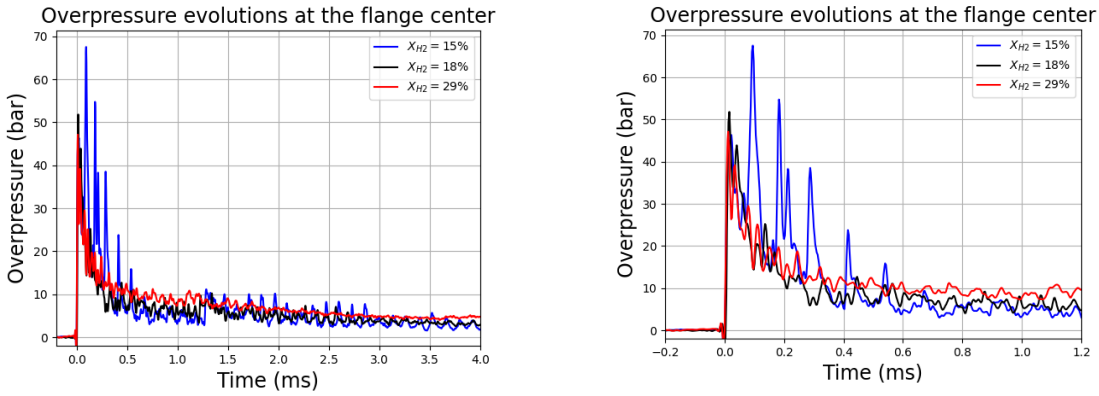

Figure 9. Overpressure evolution at the flange centre for different hydrogen concentrations (left), zoomed part of the initial time evolution (right).

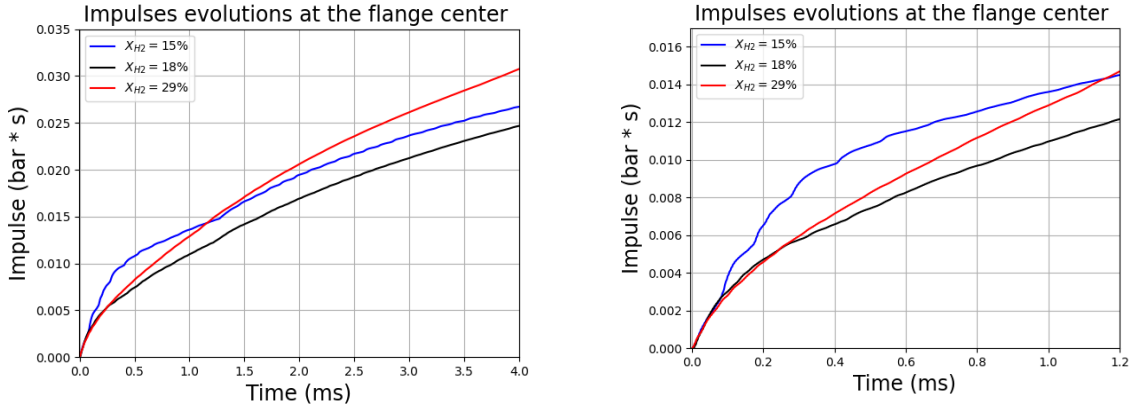

Figure 10. Impulse evolution at the flange centre for different hydrogen concentrations (left), zoomed part of the initial time evolution (right).

The presence of high-amplitude pressure peaks corresponding to hydrogen concentration of 15% (Figure 9, right) results in the highest impulse values during initial time of 1 ms (Figure 10, right). If, instead of the thick flange we had a thin metallic plate, this higher impulse would result in larger plate deformation values compare to the deformation related to stoichiometric mixture. It is shown in [3] that the deformation time of a metallic plate of 0.5 mm thickness is 0.2-0.4 ms, which is comparable to the time scale of 1 ms and explains why the lower hydrogen concentration resulted in higher plate deformation.

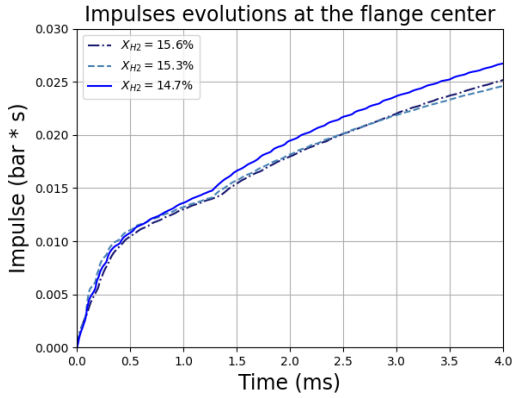

Figure 11. Impulses evolution at the flange centre for different tests. $X_{H2} \approx 15\%$.

The test with $X_{H2} \approx 15\%$ has been repeated three times and the impulse behavior is very similar for all tests (Figure 11), i.e. during 1 ms the impulse values are higher than those corresponding to the mixture with $X_{H2} \approx 29\%$.

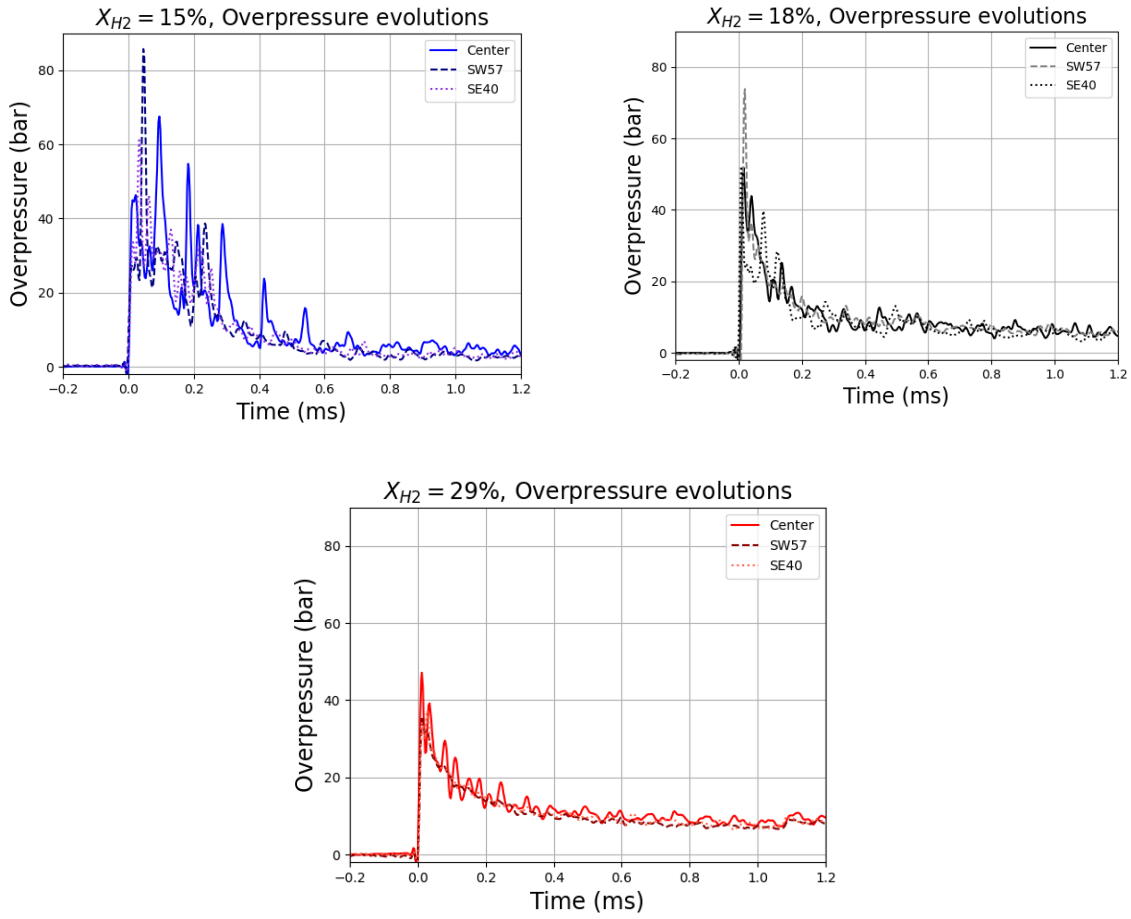

Figure 12. Overpressure evolutions at different transducer positions for hydrogen concentration of 15% (top left), 18% (top right), and 29% (bottom)

The pressure evolutions at different locations on the flange (SW57 = "South-West 57 mm", SE40 = "South-East 40 mm" from the center) are shown on the Figure 12 for the three considered hydrogen concentrations. We can see that the pressure profiles are similar for the near-stoichiometric mixture, while the pressure evolution behavior differs greatly depending on the transducer position for the mixture with $X_{H2} = 15\%$. The flame preceding shock wave arrives at the same time at all locations on the flange. Later on, 0.05-0.1 ms after the initial shock arrival, a local explosion takes place at the corner of the flange (PCB2 on the Figure 4, SW57). The resulting wave propagates to the other transducers and is reflected several times from the adapter walls.

The phenomenology of the above-described behavior is depicted on Figure 13. The shock-flame complex, propagating towards the flange separates the gas into three zones ($t = t_0^-$): the fresh unperturbed gas (upstream the shock wave), the fresh gas compressed by the shock wave (between the flame surface and the shock wave), and the burnt gas (downstream the flame surface). At time $t = t_0$ the leading shock wave arrives at the flange. The reflection of this wave leads to increasing pressure and temperature inside the fresh gas behind the reflected shock, which can result in formation of an auto-ignition hot spot in this zone ($t = t_0^+$). We mention that similar behavior was observed experimentally in [8] where stoichiometric propane-oxygen mixture was used at sub-atmospheric conditions.

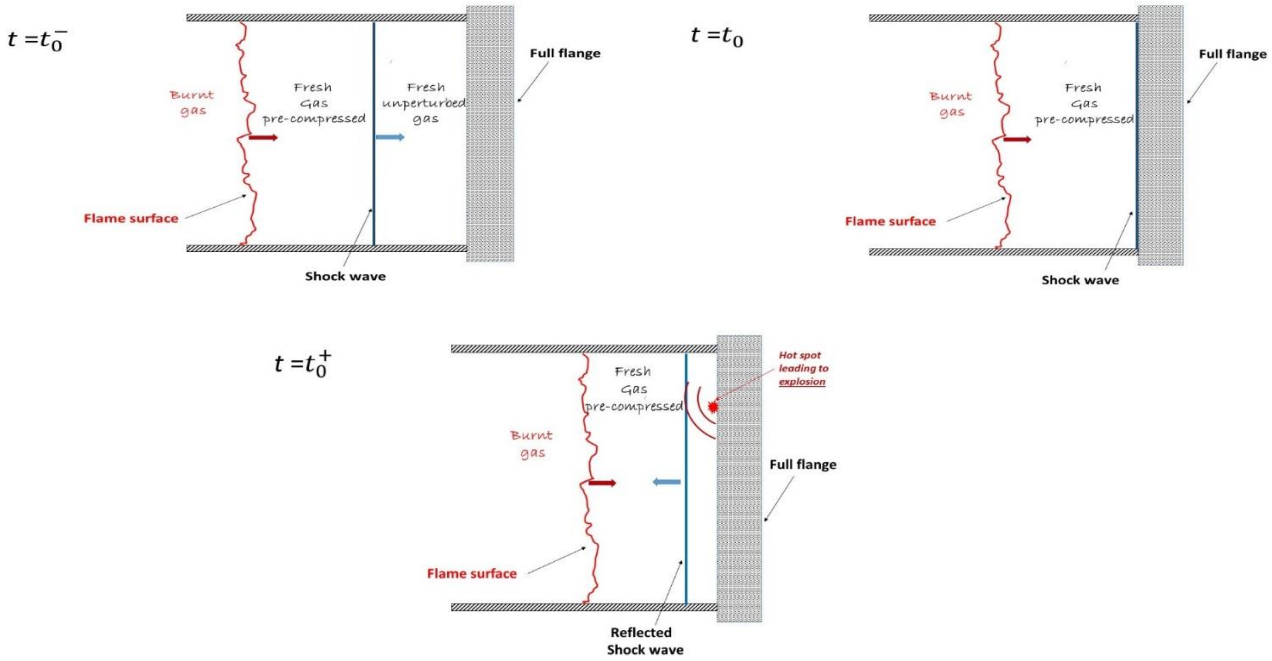

Figure 13. Sketch of the flame-shock complex propagating towards the solid flange.

The pressure evolution shows different behaviour for near stoichiometric mixture. In this case, the detonation wave propagates towards the flange and the reflected shock wave propagates inside burnt gas. The CJ detonation overpressure is $\Delta P_{CJ} = 14.6$ bar, while the theoretical value of the reflected overpressure is $\Delta P_{CJ} = 46$ bar shortly after reflection.

The overpressure generated at the flange due to combustion of the mixture of $X_{H2} = 18\%$ (Figure 12, top right) shows that some local explosions, or shock waves focusing, take place, but their energy is not sufficient in order to generate impulses which would be sufficiently higher than those corresponding the mixture $X_{H2} = 29\%$ (Figure 12, bottom).

Pressure and Impulse evolutions at the flange: conical adapter.

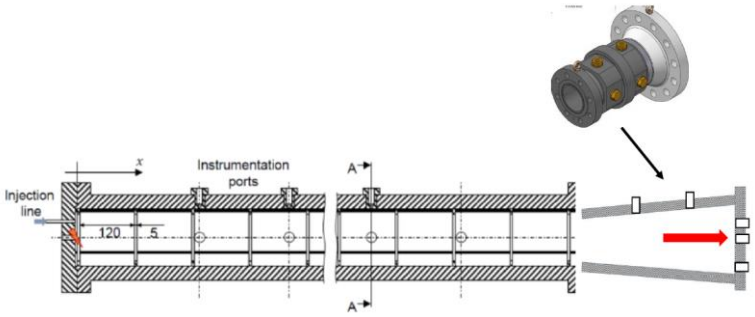

Figure 14. Sketch of the SSEXHY facility with conical adapter and a full flange equipped with pressure transducers.

The same experiments have been performed for $X_{H2} = 15\%, 18\%, 29\%$ inside SSEXHY tube equipped with the conical adapter (Figure 14). Different behaviour was observed; much lower pressure levels have been measured at the full flange transducers for the mixture containing 15% of hydrogen.

We anticipate that the shock diffraction process inside the conical adapter would weaken the incoming shock wave and, when reflected from the flange, it might not be able to ignite the pre-compressed fresh mixture layer upstream the reactive wave. Indeed, this is confirmed by experimental data. In Figure 15 we compare the overpressure signals at the flange centre; all pressure signals are shifted in time for

comparisons. We can observe a significant overpressure level reduction for $X_{H2} = 15\%$, corresponding to the conical adapter. The corresponding impulses are presented in Figure 16. We can see that the initial slope of the curves, based on the first 0.2 ms, and corresponding to the cylindrical adapter is 3.5 times larger than the slope corresponding to conical adapter (mixture with $X_{H2} = 15\%$)., while the corresponding initial slopes for the other mixtures are only 1.3-1.5 larger (cylindrical adapter) than the slopes related to the conical adapter.

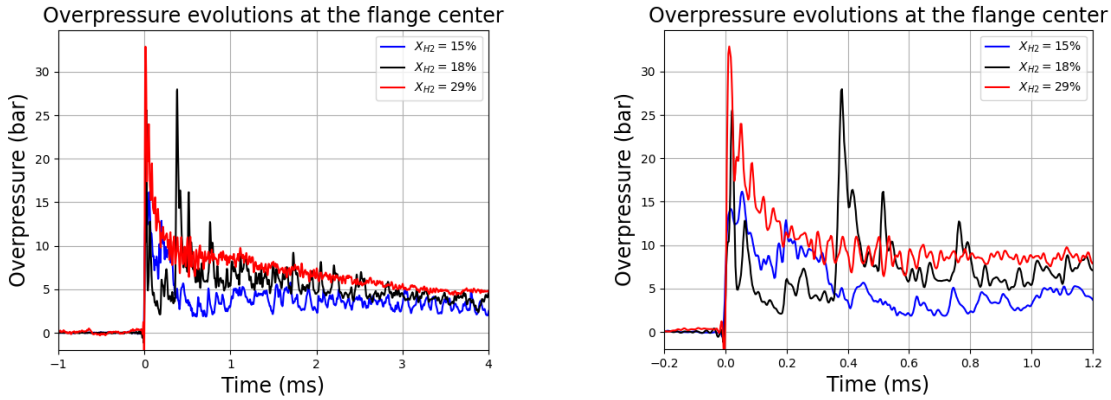

Figure 15. Overpressure evolution at the flange centre for different hydrogen concentrations (left), zoomed part of the initial time evolution (right).

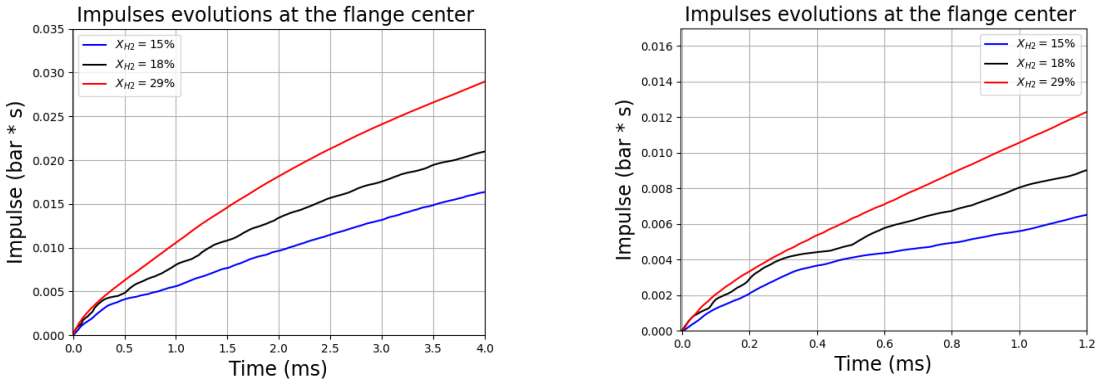

Figure 16. Impulse evolution at the flange centre for different hydrogen concentrations (left), zoomed part of the initial time evolution (right).

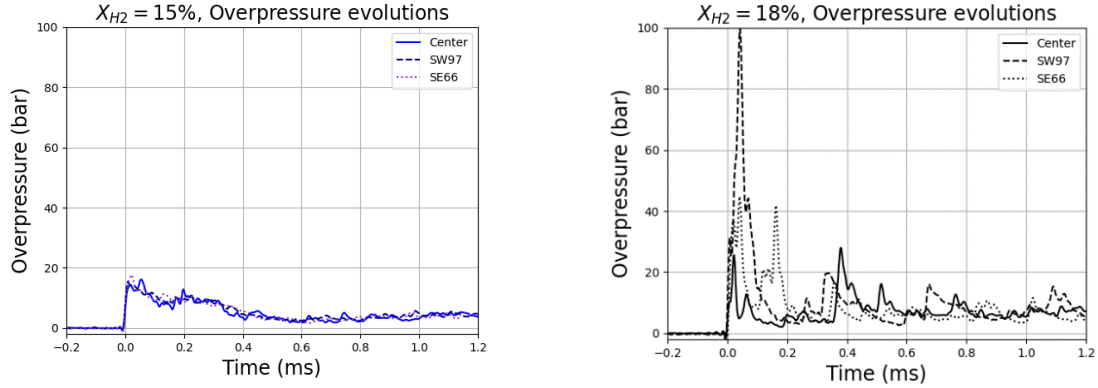

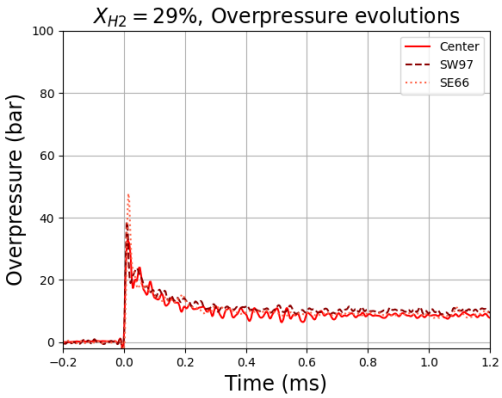

Figure 17. Overpressure evolutions at different transducer positions for hydrogen concentration of 15% (top left), 18% (top right), and 29% (bottom)

The pressure evolution behaviour corresponding to $X_{H2} = 18\%$ is very different for this configuration (conical adapter) compare to the previous configuration (cylindrical adapter). We can see (Figure 17, top right) that the overpressure is location-dependent ; large amplitude peak ($\Delta p = 100$ bar) is "seen" by the transducer SW97. At this location takes place a local explosion which propagated to the other transducers later on. Another point we would like to mention concerning this mixute, is the high dependency of the impulse evolution on the transducer location (Figure 18, left). The overpressure and impulse are much higher at the transducer SW97 which is located at the corner of the cone. This tests has been repeated twice and there is no such repeatability as was observed for the mixture of $X_{H2} = 15\%$ with cylindrical adapter (Figure 11 vs Figure 18 right). Addition tests will be performed in the near future.

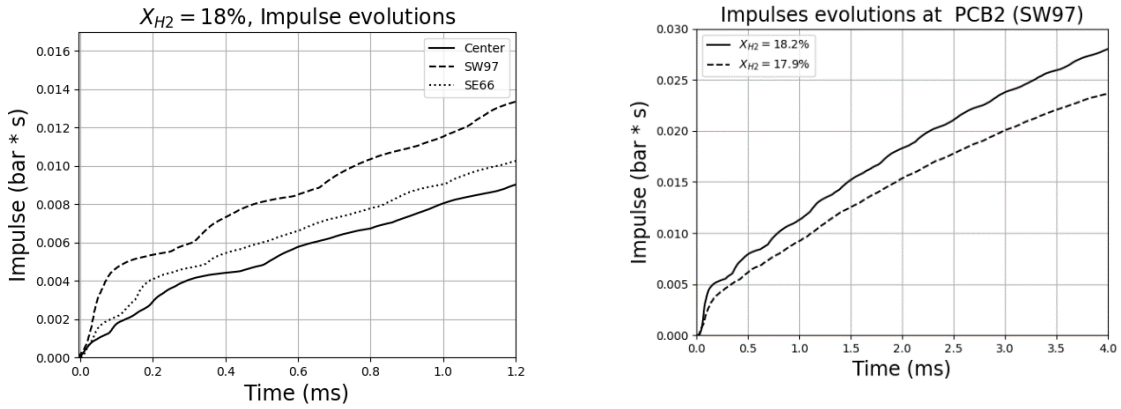

Figure 18. Impulse evolution at different transducers (left). Impulse evolutions at SW97 for different tests $X_{H2} \approx 18\%$ (right).

4.0 CONCLUSIONS AND FUTURE WORK

During previous experimental campaign performed inside SSEXHY experimental facility, it was found that high-speed deflagrations, corresponding to relatively poor hydrogen-air mixtures, resulted in higher specimen deformation compared to those related to detonations of nearly stoichiometric mixtures [3]. In order to explain this phenomenon, a separate set of experiments where a solid flange of 5 cm thickness was installed at the end of the tube. Several pressure transducers were implanted inside the flange in order to capture the time evolutions of pressure and impulse from head-on reflections for the waves corresponding to several hydrogen concentrations, $X_{H2} = 15\%, 18\%, 29\%$. Additionally, the

influence of geometry has been studied, with either elongated tube of the same diameter, or with a diverging section placed at the end of the tube where the cross-section was enlarged by a factor of 1.67. It is shown in the paper that, concerning the cylindrical adapter, the pressure and impulse evolution resulting from head-on reflection from the flange at initial times (~1 ms), have the highest values for the mixture with hydrogen concentration close to 15%. The pressure experiences high oscillations, which we attribute to the local explosions due to shock reflection inside the fresh mixture upstream of the flame. Concerning the explosions inside the tube having conical adapter, we can observe a significant overpressure level reduction for $X_{H2} = 15\%$. The overpressure/impulse levels are, on the contrary, much higher for the mixture with hydrogen concentration of 18% for this configuration. The corresponding test will be repeated in order to have sufficient statistics.
The future work will be structured around two topics: (a) additional experimental tests with the varying geometries (a cylinder of 1.3 m) and varying hydrogen concentration near the critical values, and (b) theoretical work having as a goal construction of simplified model in order to predict the overpressure/impulse behaviour inside closed volumes at head-on reflection. The latter will be performed in collaboration with Prof. M.Radulescu team of Ottawa University.

REFERENCES

[1] A. Bentaib, Meynet, N. and Bleyer, A., "Overview on hydrogen risk research and development activities: Methodology and open issues," *Nuclear Engineering and Technology*, vol. 47, no. 1, pp. 26-32, 2015.

[2] S. Kudriakov, Studer, E., Bernard-Michel, G., Bouix, D., Domergue, L., Forero, D., Gueguen, H., Ledier, C., Manicardi, P., Martin, M. and Sauzedde, F., "Full-scale tunnel experiments: Blast wave and fireball evolution following hydrogen tank rupture," *International Journal of Hydrogen Energy*, vol. 47, no. 43, pp. 18911-18933, 2022.

[3] E. Studer, S. Koudriakov, B. Cariteau and R. Scarpa, "Detailed examination of deformations induced by internal hydrogen explosions: Part 1 Experiments," in *The 8th International Conference on Hydrogen Safety*, Adelaide, Australia, 2019.

[4] R. Scarpa, Studer, E., Kudriakov, S., Cariteau, B. and Chaumeix, N., "Influence of initial pressure on hydrogen/air flame acceleration during severe accident in NPP," *International Journal of Hydrogen Energy*, vol. 44, pp. 9009-9017, 2019.

[5] R. Scarpa, Mécanisme d'accélération d'une flamme de prémélange hydrogène/air et effets sur les structures, Université d'Orléans: PhD Thesis, 2017.

[6] «Cosilab (V 4.1) Software. www.rotexo.com; 2018.».

[7] M. Kuznetsov et al., «Effect of Obstacle Geometry on Behaviour of Turbulent Flames.,» FZKA 6328 IAE-6137/3, Forschungszentrum Karlsruhe, Technikund Umwelt, 1999.

[8] W. Racotoarison, Pekalski, A. and Radulescu, M., "Detonation transition criteria from the interaction of supersonic shock-flame complexes with different shaped obstacles.," *Journal of Loss Prevention in the Process Industries*, vol. 64, 2020.